Biomass and Bioenergy 199 (2025) 107919

Contents lists available at ScienceDirect

Biomass and Bioenergy

journal homepage: www.elsevier.com/locate/biombioe

A study on the devolatilization and combustion characteristics of yak manure under simulated plateau conditions

Bin Zhao [a,b], Zihan Zhang [a], Jun Xu [b,*], Chenghong Liu [b], Mengxia Qing [a], Long Jiang [b], Yi Wang [b], Song Hu [b], Zhongyang Luo [c], Jun Xiang [b]

[a] School of Energy and Power Engineering, Changsha University of Science and Technology, Changsha, 410114, China
[b] State Key Laboratory of Coal Combustion, School of Energy and Power Engineering, Huazhong University of Science and Technology, Wuhan, 430074, China
[c] State Key Laboratory of Clean Energy Utilization, Zhejiang University, Hangzhou, 310027, China

ARTICLE INFO

Keywords:
Yak manure
Plateau area
Low pressure
Low oxygen
Particle combustion

ABSTRACT

To achieve efficient and clean utilization of biomass fuels in high-altitude regions, understanding the effects of low-pressure and low-oxygen conditions on their combustion characteristics is crucial. This study investigates the combustion characteristics of yak manure under simulated high-altitude conditions using a concentrating photothermal combustion system. A high-speed camera, thermocouples and a flue gas analyzer were employed to monitor particle behavior, temperature and flue gas components during combustion. Devolatilization products (chars) were analyzed using nitrogen adsorption/desorption, Electron Paramagnetic Resonance (EPR), and Raman spectroscopy. Results reveal that low pressure enhances the volatiles release by promoting side chain cleavage and aromatic structure formation, increases the char porosity and stable free radical concentration, and decreases the char specific heat capacity. These changes lead to higher combustion temperatures, earlier ignition and faster burnout. In contrast, low oxygen levels inhibit reactions with volatiles and char, resulting in delayed ignition and lower peak temperatures. When both low pressure and low oxygen conditions are applied simultaneously, compared to atmospheric combustion, an earlier and lower peak concentration of CO and NO emissions is detected. Additionally, slight reductions in ignition and burnout times, along with increased combustion temperatures, are observed, indicating a combined effect dominated by low pressure. These findings provide essential insights for the efficient use of biomass fuels in high-altitude regions.

1. Introduction

In high-altitude areas, energy supply is of great significance to the life of the inhabitants, and fuel combustion still plays a significant role in the energy supply modes [1–4]. As a typical plateau region, the Tibetan Plateau possesses an extensive scale of animal husbandry. The total number of domesticated yaks exceeds 13.3 million [5], and the annual production of their manure can be as high as 4.86 million tons [6]. Yak manure contains a large amount of hemicellulose and lignin, and its calorific value is higher than that of other animal manure [7–9]. Furthermore, the arid climate of Tibet results in a moisture content of less than 10 % [10], which makes yak manure an ideal fuel that farmers and herders have widely used. According to statistics, biomass, including yak manure, accounts for almost 70 % of the total energy consumption of local households [11], which can also cause a problem of environmental pollution. Considering the environmental pollution associated with traditional burning practices [12,13], it is essential to study the combustion characteristics of yak manure, which is crucial not only for understanding the combustion process but also for designing and optimizing environmentally friendly burners and advanced utilization strategies, especially at high altitudes.

Cattle manure has been extensively studied for its potential as a biomass fuel [14–19]. Researches indicate that cattle manure has a high volatile content (typically ranging from 50 % to 70 %) and a moderate ash content (approximately 15 %–35 %), with a calorific value ranging from 11.6 to 16.44 MJ/kg, making it a promising fuel source [14–19]. During combustion, the hemicellulose, cellulose, and lignin in cattle manure decompose sequentially as the conversion rate increases [18], and volatile components often ignite before the particles themselves catch fire [20]. Compared to anthracite coal, cattle manure exhibits lower ignition and burnout temperatures due to its higher volatile matter content [21]. Additionally, when mixed with textile dyeing

* Corresponding author. State Key Laboratory of Coal Combustion, Huazhong University of Science and Technology, 430074, Wuhan, Hubei, China.
E-mail address: xujun_sklcc@hust.edu.cn (J. Xu).

https://doi.org/10.1016/j.biombioe.2025.107919
Received 4 December 2024; Received in revised form 21 March 2025; Accepted 22 April 2025
Available online 27 April 2025

sludge, cattle manure demonstrates superior combustion performance, characterized by higher initial combustion temperatures, lower final temperatures, and shorter combustion durations [15]. However, most of these studies have been conducted under standard atmospheric conditions, without considering the unique environmental factors of high-altitude regions, such as low pressure and low oxygen availability. The existing findings may not fully capture the real combustion processes occurring in plateau regions, and the research for these specialized investigations under these extreme conditions is need.

Experiments simulating plateau conditions have demonstrated that low pressure significantly affects combustion temperature, radiant heat flux, and flame temperature [22–24]. For instance, under low pressure, wood ignites earlier and exhibits increased mass loss due to a lower critical heat flux density [25]. Cardboard combustion tests further revealed that low pressure attenuates solid combustion and eliminates visible flames, although smoldering persists [26]. Additionally, low pressure and oxygen levels alter heat and mass transfer between fuel particles and the environment, influencing ignition patterns and swelling behavior [27]. These studies highlight the complex and significant impact of low-pressure, low-oxygen environments on combustion processes. But the research on the combustion characteristics of cattle manure, biomass or coal under simulated plateau conditions remains very limited.

In fact, pressure is critical factor influencing fuel combustion characteristics and has been studied widely at elevated pressure range [28,29]. Studies have shown that elevated pressure significantly alters the physical and chemical properties of the char, affecting their subsequent combustion behavior [30–32]. For instance, Fermoso et al. [30] prepared and characterized devolatilized coal char at pressures of 1, 5, 10, and 20 atm, finding that increased pressure reduces volatile yield and enhances secondary tar reactions, leading to a more reactive coal char. Similarly, Zeng et al. [31] prepared chars at pressures of 1, 6, 10, and 15 atm, and observed that chars exhibited a slight increase in dissolution behavior with increasing the pyrolysis pressure. This was attributed to the faster production of volatiles within particles compared to their escape from pores, thereby influencing the subsequent combustion process. Lin et al. [32] prepared and characterized char at different pyrolysis pressures and found that the relative content of OH groups was lower at higher pressure during devolatilization, suggesting that the high pressure promoted the fracture of phenol and hydroxyl functional groups. They also found that the intrinsic reactivity of char monotony decreased with increasing pressure, similar to the changing trend of the small aromatic ring structure of char with the increase of pressure. Other studies also found that the oxygen transfer under the high-pressure conditions also play a key role on the combustion characteristics [33–35]. For instance, Li et al. [34] demonstrated that high-pressure conditions result in more pronounced combustion flames, higher char combustion temperatures, and shorter burnout times, which they attributed to improved oxygen mass transfer capacity. Yan et al. [35] studied the combustion of coal and biomass under pressurized conditions, revealing that while pressurization increases combustion rates, it can also delay ignition. They concluded that higher pressure has dual effects on combustion characteristics, promoting combustion while simultaneously inhibiting oxygen diffusion. These studies demonstrate that pressure significantly influences volatile release, char structure, combustion reactivity, and oxygen transfer, thereby affecting the combustion characteristics of fuels. These factors provide a critical foundation for further research into the combustion behavior of granular yak manure under simulated plateau conditions.

This study systematically investigated the devolatilization characteristics and combustion behavior of granular yak manure under varying pressure and oxygen partial pressure conditions using a novel concentrating photothermal combustion experimental system. The study provides a comprehensive analysis of pressure-dependent transformations in char structure, including carbon skeleton evolution, stable free radical, and pore structure development during devolatilization. High-speed imaging and real-time temperature monitoring were employed to capture particle behavior, and the ignition characteristics were mainly revealed. Furthermore, the distinctive effects and underlying mechanisms of low-pressure and low-oxygen environments on the combustion process were systematically explored, advancing the understanding of biomass fuel utilization in high-altitude conditions.

2. Methodology

2.1. Material and sample preparation

The raw Yak manure was collected from Ali Chabu Township in the Ali Region of Tibet at an elevation of 4566 m altitude above sea level. In the real applications, yak manure is usually pie-shaped with a size of 150–300 mm in diameter and 10 mm–30 mm in height [12]. It is air dried, just natural fragmentation or simply broken into a few pieces before using as a traditional fuel for home heating and cooking. So, in real applications, the pretreatment of the yak manure is rather crude and also the size is big, which makes it difficult to quantitatively study the effects of pressure and oxygen concentration on its combustion characteristics. Therefore, in this study, the raw yak manure was first pulverized to the powder with a size between 125 and 212 μm to ensure relative homogeneity of the samples, reducing its effects on the combustion. Then the sample was pressed into cylindrical pellets with a size of approximately 6.47 mm in diameter and 2.5 mm in height as shown in Fig. 1, which is roughly reduced in proportion to the actual size (assumption: the pie-shaped yak manure is 200 mm in diameter and 20 mm in height, and it is simply broken into 4 pieces when sent to the combustion boiler). By this pretreatment, the sample can be suitable for the precise combustion system to investigate the detailed combustion mechanism, and is also very important for the meaning of the current study to guide the real applications. The Proximate and ultimate analysis and the heating value of the yak manure powder samples were tested and the results are shown in Table 1. During pelleting, for each particle, yak manure powder weighed 0.1050 ± 0.0020 g was used and a forming pressure of 10 MPa was adopted. Further, a 1 mm hole was meticulously drilled into the center of each particle to enable suspension in the reactor.

2.2. Concentrating photothermal combustion experimental system

To simulate the high heating rate typical of yak manure combustion, minimize the impact of secondary reactions, and enable multi-parameter real-time monitoring of the particle combustion process, combustion experiments were conducted using a concentrating photothermal particle combustion system as depicted in Fig. 1. This system mainly comprises four distinct modules: a gas supply unit, a heating reactor, a vacuum control apparatus, and a data acquisition module. The gas supply component governs the flow rate and the oxygen concentration of the gas supplying into the reactor. During the experiment, a vacuum pump was used to adjust and maintain a constant pressure inside the reactor to replicate the low-pressure environment found in plateau regions. The main pressure reducing valve is adjusted to the same number as the vacuum regulating valve to adjust the vacuum level in the reactor and to ensure a stable pressure in the combustion zone. The reaction system is tested for airtightness before the experiment to prevent outside gases from entering the reactor and affecting the gas ratio. The core of the heating module features a stainless-steel reactor ($60 \times 60 \times 90$ mm) housing two halogen tungsten lamps (24 V/250 W), each with a power supply. Adjustments in the voltage achieved variations in energy input to the reactor. The reactor has transparent quartz windows on all sides to transmit light and enable visual observation. A tar cooling unit and gas filtration system were positioned at the reactor outlet to condense moisture and tar from the gas, preventing vacuum pump blockages. A thermocouple was used to monitor internal temperatures of particle, which were logged onto a data recorder (NI cDAQ-

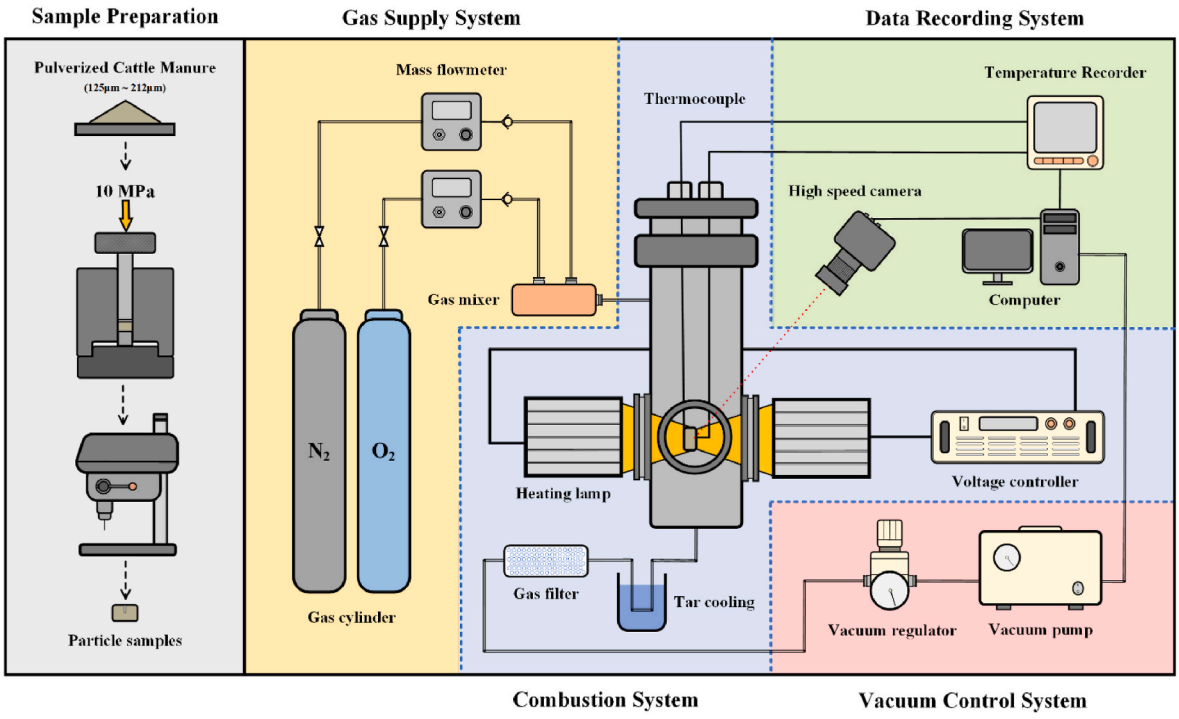

Fig. 1. The schematic diagram of the sample preparation process and the concentrating photothermal combustion experimental system.

Table 1
Proximate and ultimate analysis of dried yak manure.

Sample	Proximate analysis[a] *wt.*/%				Ultimate analysis[b] *wt.*/%					HHV MJ·kg^{-1}
	A	V	FC[c]	M	C	H	O[c]	N	S	
Yak manure	27.27	51.78	13.31	7.64	33.24	4.29	30.90	1.82	0.22	13.37

[a] Air dry basis.
[b] Dry basis.
[c] Calculated by difference.

9174). Capturing real-time combustion dynamics was achieved through a high-speed camera (PHOTRON FASTCAM UX-50), which recorded dynamic visuals through the reactor's front glass window. In addition, a flue gas analyzer (MRU NOVA-PLUS) connected to the end of the vacuum pump was used for real-time monitoring of the emission volume fraction of CO and NO during the experiments. This multifaceted approach ensured accurate and instantaneous measurement of crucial parameters throughout the experimental process. More details about the temperature control for the concentrating photothermal combustion experimental system can be referred to our previous studies [36,37]. In order to study the combustion process of yak manure at different altitudes, we selected three pressure conditions in China: 4500 m above sea level in Ali, Tibet (about 0.05 MPa), 2300 m above sea level in Xining, Qinghai (about 0.075 MPa), and 100 m in Wuhan, Hubei, (about 0.1 MPa). It must be pointed out that in the atmosphere below 8000 m altitude above sea level, the volume fraction of oxygen usually remains around 20 %. However, as altitude increases, the thinning of the atmosphere leads to a decrease in the absolute oxygen content. To more accurately represent the number of oxygen molecules flowing around the particles, the partial oxygen pressure in the air can be calculated using Dalton's law of partial pressures as equations (1) and (2). When the oxygen partial pressure in the reactor remains constant, it can be assumed that a certain number of oxygen molecules flow around the particles, thus more accurately representing the tendency of the oxygen content to decrease with increasing altitude. Low oxygen conditions throughout this paper denote low oxygen partial pressure conditions.

$$P = \sum_{i=1}^{n} P_i \tag{1}$$

$$P_{O_2} = P \cdot x_{O_2} \tag{2}$$

P is the total pressure, P_{O2} is the oxygen partial pressure, and x_{O2} is the oxygen to air ratio. Since the above gases are approximate ideal gases, the ratio of the number of substances can be approximated to the volume fraction. So, the three conditions had partial oxygen pressures of 0.01 MPa, 0.015 MPa, and 0.02 MPa, respectively. The experimental conditions recorded are the total pressure in the reactor (P) and the partial pressure of oxygen (P_{O2}). To distinguish between pressure and oxygen content conditions in each experimental condition, the experimental condition was recorded as total pressure (P)-partial pressure of oxygen (P_{O2}) in the reactor, e.g., 0.1–0.02 indicates a total pressure of 0.1 MPa and a partial pressure of oxygen of 0.02 MPa in the reactor. In these experiments, the settings were set up to have total pressures of 0.1 MPa, 0.075 MPa and 0.05 MPa and partial pressures of oxygen of 0.02 MPa, 0.015 MPa and 0.01 MPa in the reactor, respectively. The actual working conditions were labeled (Condition series d), when the pressure and partial pressure of oxygen were reduced in the same proportions. The low pressure condition (Condition series b) and low oxygen partial pressure condition (Condition series c) were also set to better reveal the independent effects of pressure and oxygen content on the combustion process at high altitude. In addition, pyrolysis conditions at different pressures are set up (Condition series a) to investigate the effect mechanism of pressure on the devolatilization process under a 1000 mL/min

nitrogen atmosphere. In these experiments, the voltage was set to 20 V, the radiated heat from the two lamp cups was about 370 J/s, and the vacuum regulating valve was set to 0.1 MPa, 0.075 MPa, and 0.05 MPa, respectively. To investigate the structure evolution characteristics of char during the devolatilization process, the reaction was interrupted at the moments of 5 s, 10 s, 15 s, 20 s, 30 s, 60 s, 90 s, 120 s, and 150 s in the devolatilization experiments and the char particles were collected for the further characterization.

2.3. Characterization of the char structures

Raman spectra of the chars were obtained in a micro-Raman spectrometer (Thermofisher DXR2). The laser power was controlled at 1 mW to reduce the thermal damage. In order to reduce the errors caused by the heterogeneity of the biochar, all tests were performed in a mapping mode according to our previous studies [38]. This method tested more than 20 points for each sample, and the average spectrum was calculated and used for further structure analysis. Raman bands in the range of 800–1800 cm^{-1} are related to the structure of the carbon skeleton of organic matter. The common Raman spectroscopy deconvolution analysis methods include ten bands method and five bands method. Generally, the five bands method is mostly used for materials with high graphitization degree [39,40]. This study involves the structural evolution throughout the entire devolatilization process of the material; thus, the ten bands method is used for Raman spectral analysis according to Li et al. [41] and our previous studies [42,43]. Fig. S1 shows A sample of ten band method for data processing of the Raman spectrum. The results include the band (R, S_R, S, S_L, D, V_R, V_L, G_R, G, G_L bands, and shown in Table S1). It was found that the D band can mainly represent the condensed extensive aromatic ring system (not less than 6 rings) in char. The G band can be mainly attributed to the aromatic ring quadrant breathing for low graphitization degree carbon materials [44]. Therefore, A_D/A_G can partially reflect the relative content of ordered rings (large aromatic rings) in char [43].

The characteristics of the stable free radical in the chars was measured by an Electron Paramagnetic Resonance (EPR) spectrometer (Bruker MS5000), the same with our previous studies [38,45]. The magnetic field range was set to 320–350 mT with the center field at 335 mT. The scanning width was 10 mT, and the scanning time was 60 s. The concentrations of stable free radicals were calculated based on the double integral of the EPR spectrum. The g values of the biochar were calculated to reflect the type of stable free radicals according to our previous studies [38]. The g value was calculated as follows:

$$g = \frac{h\nu}{\mu_B B_r} \tag{3}$$

Where h is Planck's constant, ν is microwave frequency, μ_B is the Bohr magnetron and B_r is the magnetic strength. The magnitude of the g factor can represent the type of free radicals, and according to the study, when the g factor is between 2.0030 and 2.0040, the free radicals are mainly in the form of a mixture of oxygen- and carbon-centered radicals. When the g factor is larger than 2.0040 and less than 2.0030, the free radicals in biochar are mainly centered on oxygen atoms and carbon atoms, respectively [38].

The char's specific surface area and pore volume were tested by nitrogen adsorption/desorption (JW-BK200A, JWGB) and calculated according to the BET and BJH methods [46,47]. Given the wide range of pore size distribution of this sample, the pore size distribution curve used in this study is dV/dlogD, where V represents pore volume and D represents pore diameter.

3. Results and discussion

3.1. Image characteristics of the particles during devolatilization and combustion

The pictures of the devolatilization and combustion process of yak manure particles under different conditions are shown in Fig. 2. As can be seen from all these figures, both the devolatilization and combustion processes can be divided into three stages. Stage I is the temperature rapidly rising section. In this stage, the light source begins to illuminate the particles, and there is little observable change. This stage is very short and continues for approximately 2–3 s. Then, large amounts of "smoke" are released from the surface of the particles, which can be marked as stage II. In this stage, a significant release and oxidation of volatile components occurs, and it can continue even for about 20 s. Following the release and oxidation of the volatile, char particle can be clearly found and continues for tens of seconds, which can be marked as stage III. In this stage, the char aromatization occurs during the devolatilization as the char particle is dark, and char oxidation occurs with a noticeable increase in the brightness of the char during combustion conditions. So, it can be distinguished the char aromatization or combustion from the brightness of the char in this stage. It needs to point out that, in Stage II, large amount of volatiles release from and around the particle, it can be very hard to confirm when the volatile or the char ignition, which will be further analyzed combing the particle temperature in Section 3.3.

As shown in Fig. 2, it can be also seen that the stage II of the particles during devolatilization is significantly longer than the same stage of the combustion process. It suggests that the release of the volatiles can be also affected by oxygen content in the atmosphere. Oxidation or combustion of the volatiles can accelerate their release. Besides, as the total pressure decreases from 0.1 MPa to 0.05 MPa, the duration of stage II also decreases. While, when the partial pressure of oxygen decreases, the duration of stage II is reversed. When the pressure and oxygen partial pressure were simultaneously reduced, as shown in Fig. 2(d), the reduction was less than when only the total pressure was reduced. This indicates that the decrease in oxygen partial pressure increases the duration of the volatile release and makes the release and combustion of volatiles more difficult. The results illustrate that changes in oxygen levels and atmospheric pressure can significantly impact the combustion process.

To quantitatively characterize the processes depicted in Fig. 2, we define the t_{delay} (devolatilization delay time) as the duration between a particle's exposure to the light source and the onset of volatile release, and the $t_{duration}$ (devolatilization duration) as the time from the start of volatile release to their complete disappearance within the reactor. The results of the t_{delay} and $t_{duration}$ for all the conditions are shown in Fig. 3. From Fig. 3(a), it can be observed that as the environmental pressure decreases, both the delay time and the duration of volatile components decrease. When maintaining a constant oxygen partial pressure inside the reactor, the total pressure drops from 0.1 MPa to 0.05 MPa, the duration of volatile component removal decreases significantly from 18.9 s to 13.7 s, marking a substantial reduction of 27.51 %. From Fig. 3 (b), it can be observed that as the oxygen content in the environment decreases, the delay time of volatile compounds continues to decrease, but the duration of volatile compounds increases from 18.9 s to 26.3 s, representing a growth of 39.15 %. When both factors decline simultaneously, as shown in Fig. 3 (c), the t_{delay} and $t_{duration}$ of volatile components both decrease. However, the reduction is less pronounced compared to Fig. 3 (a), with a decrease of only 5.29 %. This phenomenon indicates that the release of volatiles is facilitated under low-pressure conditions and the low oxygen condition can increase the duration of the volatile release process. In a low-pressure environment, there is a significant pressure difference between the interior and the surroundings of the particles, making it easier for volatiles to be released. On the other hand, in an oxygen-containing environment, the oxygen can react

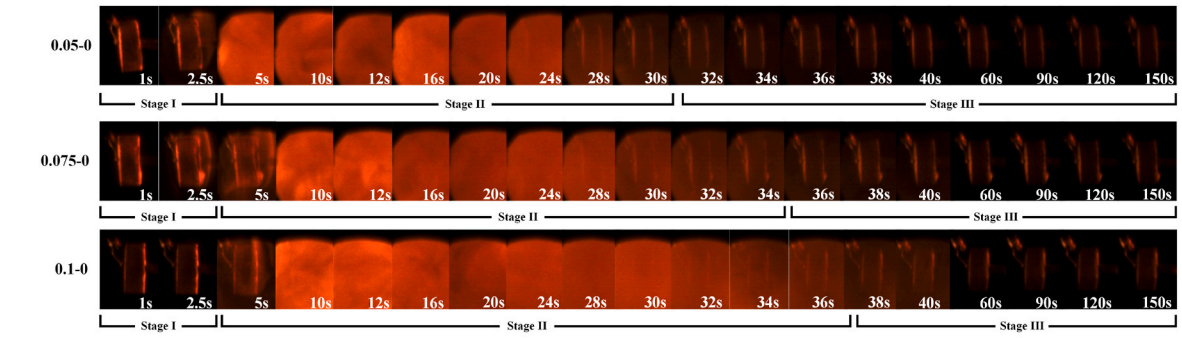

a) Devolatilization process of yak manure at low-pressure conditions.

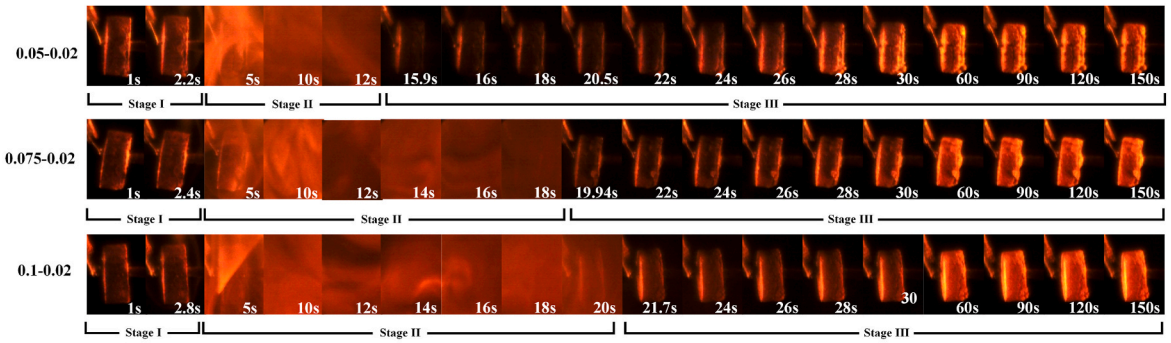

b) Combustion process of yak manure at low pressure conditions.

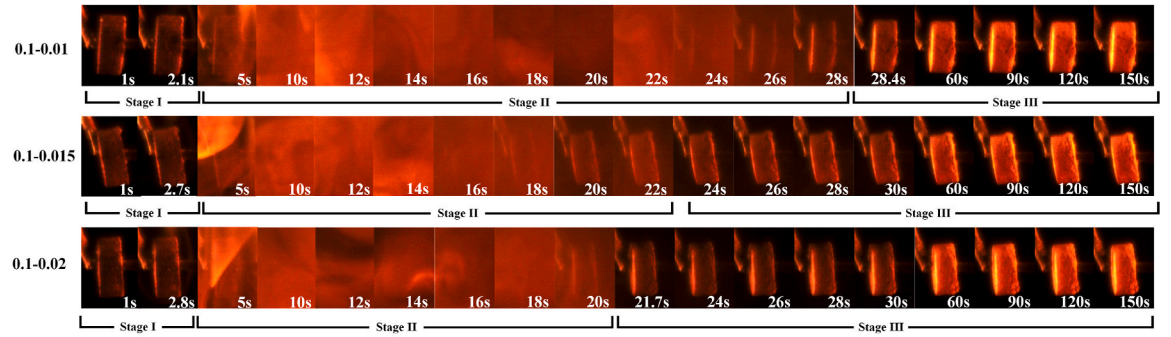

c) Combustion process of yak manure at low oxygen conditions.

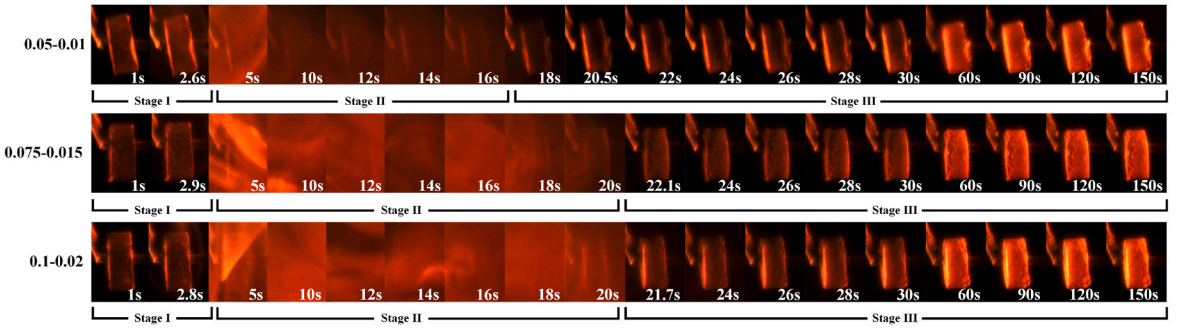

d) Combustion process of yak manure at low pressure and low oxygen conditions.

Fig. 2. Devolatilization and combustion process of yak manure particles under different conditions.

with the volatiles and further speed up the release and consumption of the volatiles. When the oxygen partial pressure in the atmosphere decreases, the supply of oxygen is limited, reducing the consumption rate of volatiles around the particle, thus decreasing the speed-up degree for the release and consumption of the volatiles. Therefore, under conditions of both low pressure and low oxygen, two opposite effects take place. As a compromise reduction for the duration of volatile release is observed under both low pressure and low oxygen condition, it indicates that the promoting effect of low pressure on volatile release is more pronounced than the effects of low oxygen.

The swelling characteristics of yak manure particles during the devolatilization and combustion processes are illustrated in Fig. 4. From Fig. 4, it can be seen that in all four sequential conditions, the swelling rate of the particles increases slightly at Stage I, then decreases sharply

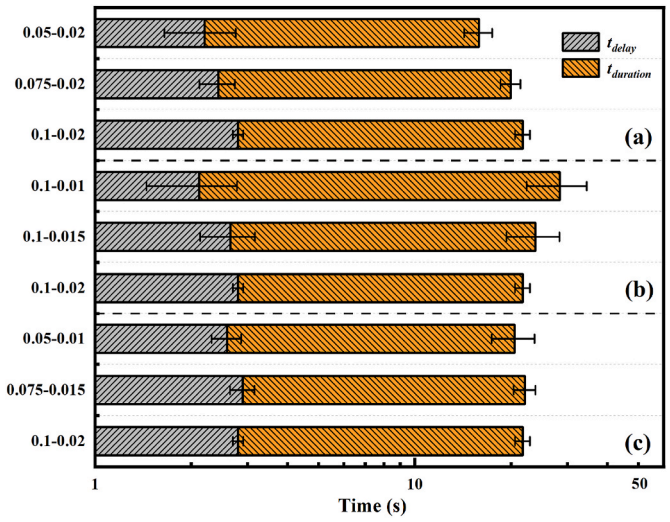

Fig. 3. Devolatilization delay, devolatilization duration of yak manure particles during combustion.

when the particles experiences Stage II, and finally decreases slowly in Stage III. At the initial Stage I (about 0–2.5 s), the particles expand due to heating, causing an expansion of the particle and an increase in particle volume. At intermediate Stage II (about 2.5–30 s), a significant release of volatile components from the particles rapidly reduces particle volume. At the late Stage III (about 30–150 s), the continuous combustion of char causes a slight decrease in particle volume. It should be noted that the particles still maintain quite large particle morphology in the later stage of combustion due to the high ash content in the char particle.

In the N_2 atmosphere in Fig. 4(a), the particles' volume decreases as the pressure decreases, especially for the particles after Stage II. This is mainly because the pressure gradient inside and outside the particles at low pressures increases the ability of volatiles to precipitate outward, promoting the release of volatiles and weakening the effect of volatiles on the particle volume. This highlights the critical effects of pressure on the devolatilization process and explains the phenomenon of low swelling ratios at low pressures exhibited in Fig. 4(b) and (d). It is noteworthy that the expansion tendency of the particles changes when oxygen is present in the atmosphere as shown in Fig. 4(a) and (b), and it is clear that oxidation reaction of the volatile or char indeed affects the volume size of the particles. This may be due to the different mechanisms by which pressure and oxygen influence the swelling characteristics of the particles, resulting in the existence of the optimum value of the swelling ratio of the particles. In addition, as shown in Fig. 4(c), the variation of the particle swelling ratio decreases with the decrease of oxygen partial pressure. It is tiny in the deficient oxygen partial pressure environment. It indicates that the partial pressure of oxygen in the environment has a limited effect on particle swelling. In contrast, the swelling characteristics are strongly influenced by the volatile release rate in the particles.

3.2. *Effects of the pressure on the char structure evolution during devolatilization*

3.2.1. *Char yield*

The char yield of yak manure at different pressures during devolatilization is illustrated in Fig. 5. It is evident that the weight loss of particles primarily occurs within 5–30s, accounting for approximately 90 % of the total particle mass loss. With a decrease in pressure, the char yield of the particles also decreases. It indicates that the lower the pressure of the condition, the more significant the amount of volatiles released from the particles. The difference between the char yield at 0.05Mpa and 0.1Mpa can be more significant than 5 %. This phenomenon can be mainly attributed to two main factors. Firstly, the volatile components in yak manure particles diffuse from the insides of the particles more easily under low-pressure conditions, which shortens the residence time of the volatiles in the char. Besides, it can significantly reduce the secondary reaction between the volatiles and the nascent char, consequently reducing the quantity of generated char. These two factors produce a lower char yield for yak manure particles under low-pressure conditions. It needs to point out that the difference in the char yield between various pressure conditions decreases with the continuing of the thermal dealing and the char yield nearly almost the same after 30s, which can be mainly attributed to the further release of the volatile and the broken of the cross-link structures forming during the secondary reaction between the volatiles and the nascent char at

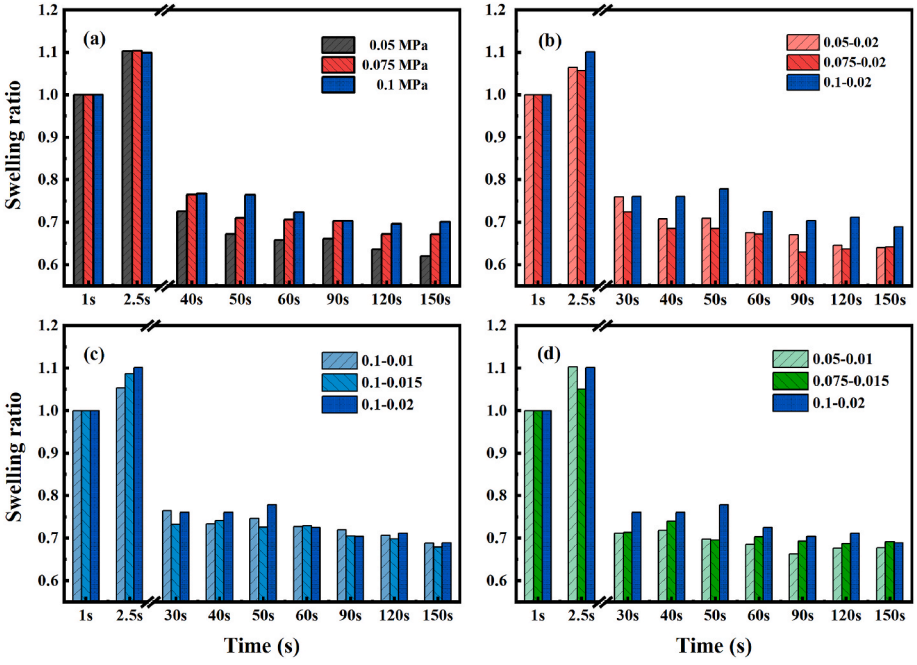

Fig. 4. Swelling ratio of yak manure particles during pyrolysis and combustion.

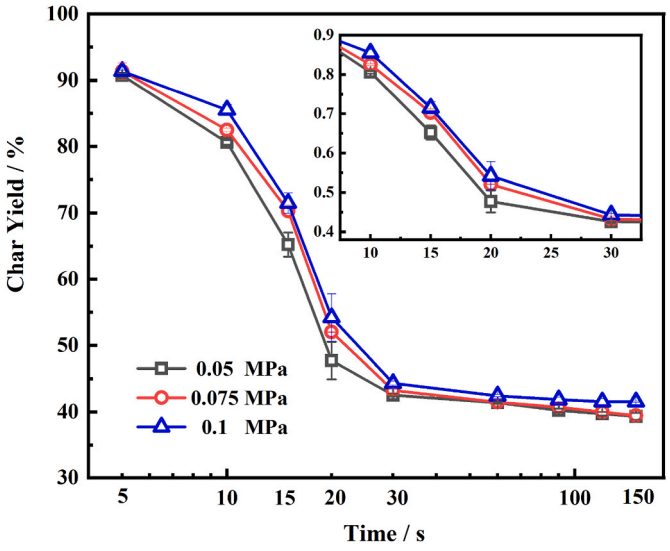

Fig. 5. Char yield of yak manure at different pyrolysis pressures.

higher pressure condition. How the accelerated release of the volatiles affects the char structures and combustion characteristics is worthy of further study.

3.2.2. Evolution of the carbon skeleton structure during devolatilization

Fig. 6 shows the changing trend of the chars' Raman band area ratio A_D/A_G during the devolatilization process of yak manure at different pressures. As the devolatilization process proceeds, the ratio of A_D/A_G of the char decreases between 0 and 15 s. In this stage, a large amount of volatiles releases from the char. Yak manure mainly consists of lignin, cellulose, and hemicellulose. So, the number of aromatic rings in raw yak manure is limited []. Under heating, except for the rapid release of volatiles, alkane, olefins can translate into aromatic hydrocarbon, tiny aromatic rings. Therefore, in this stage, the ratio of large aromatic rings in the aromatic hydrocarbon rapidly decreases. Besides, as the pressure decreases, the ratio of A_D/A_G increases in this stage. It is mainly because more volatiles components that are mainly alkane and olefins or small aromatic rings remain in the char, forming more small aromatic rings for higher pressure conditions [43], which can result in a lower value of A_D/A_G.

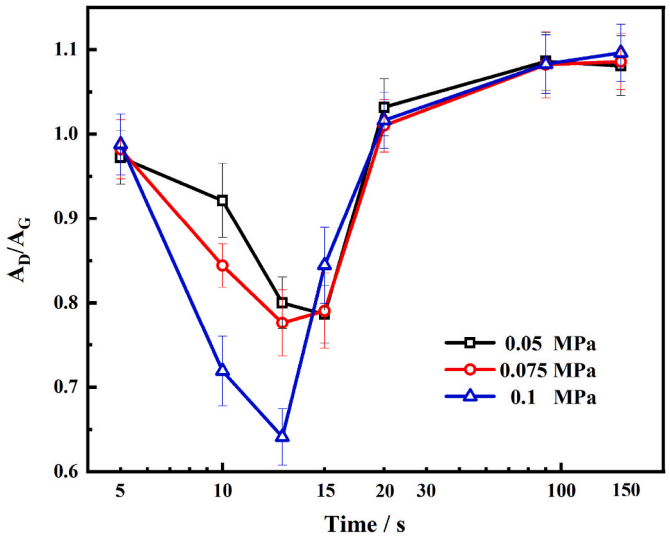

Fig. 6. Carbon skeleton structure evolution of yak manure under different pressures.

With the devolatilization process proceeding further, the A_D/A_G of the char increases from a decrease between 15 s and 20 s. From the results of the char yield, it can be known that this stage is between the middle and the later stages of the devolatilization process. It means a fair number of volatiles are still released from the char after this stage. It is known that these volatiles/tars would probably form more through the breakage of aliphatic structures or the loss of alkyl-substituted attached to the original aromatic rings with little effect on the original aromatic rings in the char [48]. Thus, the small aromatic rings combine to form larger aromatic rings, which also start to significantly take place in this stage, increasing the A_D/A_G. It must be pointed out that the larger the pressure, the larger the increase. This is mainly because for the chars under high pressure, the release of the volatiles is slower, and volatiles continue to form and release from the char. During this process, the newly forming volatiles can combine with the volatiles/tar that remain in the char, forming larger aromatic rings. In the later stage of the devolatilization process, the release of the volatiles is finished. The condensation of the aromatic rings mainly takes place. Thus, the A_D/A_G of all the chars increases rapidly. Besides, the A_D/A_G for the chars formed under different pressures in this stage has no noticeable discrepancy. It indicates that the pressure mainly affects the char structures in the volatile release stage, and these differences are reduced as condensation takes to a great degree.

3.2.3. Evolution of the stable free radicals in the char during devolatilization

Fig. 7 shows the change trends of the concentration (Fig. 7(a)) and the g value (Fig. 7(b)) of the stable free radicals in the char during the devolatilization process of yak manure. From Fig. 7(a), with the devolatilization process, the concentration of the stable free radicals in the char increases rapidly, reaching the maximum value at 20 s, and then rapidly decreases. The increased process of stable free radicals mainly corresponds to the primary process of the release of volatile. It is known that the formation and release of volatiles is a free radicals' reaction process, in which the bonds break, forming many free radicals [45]. Some of them release from the char, and another part can remain in the char, such as the broken side bond of the aromatic rings. In this process, most of them rapidly annihilate each other as they are very active. However, some of them can be stabilized due to the space steric hindrance effect of the molecular network of char [49]. So, it also confirms that the significant condensation of the aromatic rings takes place after 20 s, during which, the stable free radicals eventually annihilate as the shrinking distance between macromolecules increased. At the same time, it shows an interesting phenomenon that the concentration of stable free radicals initially increases and then decreases with the extension of pyrolysis time, while the carbon skeleton structure parameter A_D/A_G first decreases and then increases. This suggests a significant correlation between the changes in the biochar's carbon backbone structure and the generation of stable free radicals. In the early stages of devolatilization, covalent bonds in substituents such as C-O, methylene and methyl groups gradually break, forming free radical fragments. These free radical fragments interact with each other and form new chemical bonds due to their high reactivity, releasing small molecular compounds and participating in the synthesis of small aromatic ring structures. As a result, the concentration of stable free radicals increases during this stage, while A_D/A_G decreases. However, in the later stages of devolatilization, aromatic rings undergo condensation, leading to a significant increase in the formation of large aromatic ring structures. With the enhancement of their stability, the concentration of stable free radicals gradually decreases. Additionally, the compression of the carbon backbone structure increases the chances of annihilation between stable free radicals, further accelerating the decrease in free radical concentration. Consequently, in this stage, the free radical concentration decreases while A_D/A_G increases. Thus, it is evident that the evolution of the carbon skeleton structure and the generation of free radicals are closely related, and their interactions play a crucial role in

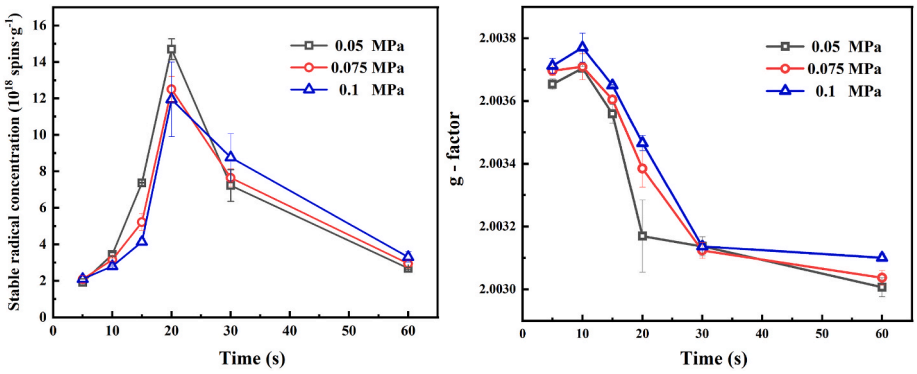

(a) stable radical concentration (b) g-factor

Fig. 7. Changes of the stable free radical during devolatilization under different pressures.

the pyrolysis process.

As shown in Fig. 7(b), the g factor of the stable free radicals exhibits a trend of initially increasing and then decreasing with the progression of devolatilization time. Notably, the g factor increases during the first 10 s of devolatilization and decreases thereafter. The g factor of stable free radicals is indicative of their type, and when the g factor falls within the range of 2.0030–2.0040, it typically reflects the presence of a mixture of carbon-centered and oxygen-centered radicals. Smaller g factor suggests higher relative abundance of carbon-centered radicals. The results in Fig. 7(b) further suggest that the decomposition of oxygen-containing functional groups and side chains, such as C=O and O-H during the early stages of pyrolysis, leads to the generation of oxygen-centered radicals, which are retained within the internal structure of the char. At the same time, the formation rate of carbon-centered radicals is relatively slow during this stage. As a result, the stable free radical characteristics in the initial pyrolysis phase are predominantly influenced by oxygen-centered radicals, which is reflected in the observed increase in the g factor. As the devolatilization process continues, it can be seen that the g-factor continually decreases with the increase of the devolatilization degree. This suggests that as the devolatilization degree

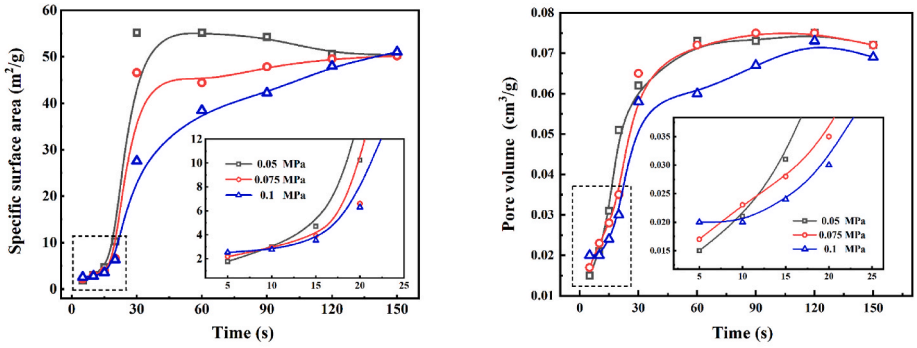

(a) specific surface area (b) pore volume

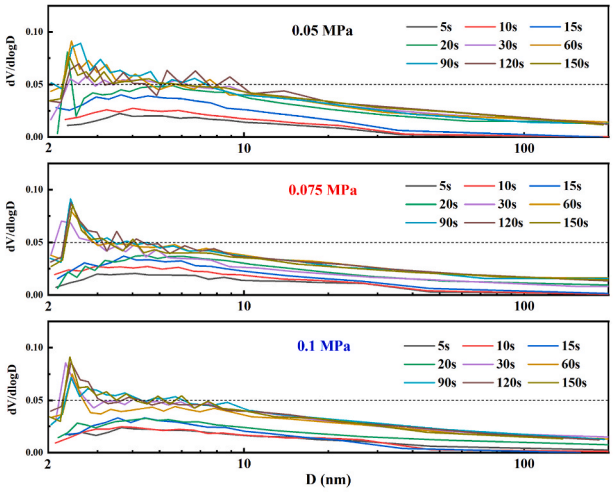

(c) pore size distribution of yak manure at different pressures and different time

Fig. 8. Pore structure evolution of yak manure under different devolatilization pressures.

increases, there are more carbon-centered radicals, attributable to the release of oxygen atoms from the char. Additionally, higher pressure conditions result in elevated g-factors for the char. This indicates that pressure during the devolatilization process at low temperatures also influences the types of radicals. This can be attributed to the fact that under higher pressure, a greater quantity of volatiles/tar containing more oxygen-centered radicals tends to remain in the char, contributing to the formation of the char with a higher concentration of oxygen-centered radicals.

3.2.4. Evolution of the pore structures in the char during devolatilization

Fig. 8 shows the change trends of the specific surface area (Fig. 8 (a)), pore volume (Fig. 8 (b)), and pore size distribution (Fig. 8 (c)) during the devolatilization process of yak manure. As shown in Fig. 8 (a), the specific surface area of the pore structure in yak manure gradually increases before 15 s. It then rapidly increases within 15–30 s as the devolatilization process proceeds. As pressure decreases, the growth rate of the pore-specific surface area was accelerated in the 15–30s stage, and the specific surface area of the chars under 0.05 MPa first reaches its maximum value and then remains relatively stable. The specific surface area of the chars under 0.075 MPa and 0.1 MPa continues to increase after 30 s before eventually reaching the same maximum value as the chars under 0.05 MPa. As shown in Fig. 8(b), the changing trend of the pore volume for the char particles is similar to the specific surface area. It increases with the increase of the devolatilization time, and the increasing rate rises with the decrease in pressure. From the pore size distribution shown in Fig. 8(c), it can be seen that before the 20 s, during the devolatilization, the pores with a size between 2 nm and 30 nm all had a mild increase. After 20 s, the pores between 2 and 3 nm significantly increase. These results indicate that more and more pores form during the devolatilization process. Combing with the devolatilization process image (Fig. 2) and char yield (Fig. 5), it can be known that the number of pores between 2 nm and 50 nm all increases in the early stage of the devolatilization process, and the pores with the size less than 10 nm especially less than 3 nm mainly form in the later stage of the devolatilization process, which makes the significant contribution for the increase of the specific surface area and pore volume [50]. It indicates that the rapid release of the volatiles can promote the formation of pores with a wide range of sizes, and the aromatization of the char in the later stage of devolatilization mainly takes place, which has a significant contribution to the formation of pores with smaller size.

It can also be seen from Fig. 8(c) that the number of pores between 2 and 10 nm significantly increases at 20 s for the chars formed at 0.05 MPa, earlier than that at 0.075 MPa and 1 MPa. It is consistent with the results that the release of volatiles is completed and aromatic condensation takes place earlier, and thus smaller pores are formed earlier at 0.05 MPa. It needs to point out that the number of 2 nm and 3 nm in the char prepared at 0.1 MPa is largest and the number of pores between 3 nm and 8 nm is largest for the char at 0.05 MPa at later stage of the devolatilization process. There are two main reasons for the result. One is that the release of volatiles is completed earlier at 0.05 MPa, the pore size slightly increases with the collapsing and fusing of the inter-pore spaces. The other factor is that the volatiles stay longer inside the particles, and more secondary reactions can occur under higher pressure conditions, forming some soot or small charcoal particles, thus being part of the pores, reducing the pore size, or even blocking the pores and reducing the pore volume and specific surface area [33].

3.3. Effects of the pressure and oxygen on the ignition and combustion characteristics

The changing trend of the temperature of a typical yak manure particle during combustion is illustrated in Fig. 9. The average relative standard deviation (RSD) of the particle temperature was calculated for each condition throughout the combustion process to determine the stability of the experimental system during particle combustion. The results showed that the RSD was consistently below 5 % for all operating conditions. The RSD peaks only occurred during the initial and ignition phases, indicating good repeatability of the combustion phase. The derivative of the temperature curve calculates the heating rate. As observed in Fig. 9, when the light source startes to work, the particle temperature and heating rate rapidly increases. Subsequently, a significant amount of moisture and volatile matter is released, and the heating rate decreases slightly as this process is endothermic. Following this, the volatile matter ignites and undergoes gas-phase combustion. With a large amount of heat releases during the volatile combustion, the particle's heating rate significantly increases. Additionally, the combustion of the volatile matter affects the oxygen diffusion from the outside to the char surface, preventing the char particles from igniting. As the heat released from volatile combustion decreases, the rate of rises in the temperature of the particles decreases. Char particles are ignited when there is no visible flame of the volatile, and the temperature is high

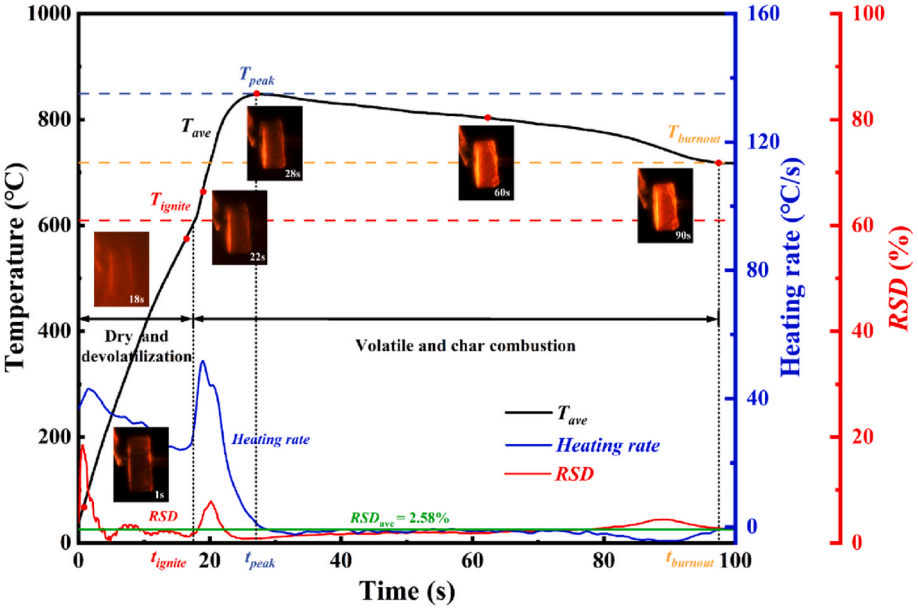

Fig. 9. Typical temperature change process of yak manure particles during combustion.

enough in the reactor. As the char oxidizes, the temperature eventually stabilizes, and the particles burn out. Based on this process, the ignition temperature of the particle ($T_{ignition}$) is defined as the point at which the heating rate significantly increases. The peak temperature of the particle (T_{peak}) is defined as the maximum temperature of the process, and the average of the particle temperature (T_{ave}) is calculated for the whole combustion process. The point when the temperature of the char particle decreases to T_{ave} again is defined as the burnout point. The times of the point for the $T_{ignition}$, T_{peak}, and burnout are defined as $t_{ignition}$, t_{peak}, and $t_{burnout}$.

Fig. 10 illustrates the temperature profile of yak manure particles during devolatilization and combustion for different conditions. As shown in Fig. 10(a), the temperature of the particles increases rapidly upon the application of the light source and eventually stabilizes. With the decrease of devolatilization pressure, the temperature of the particles increased from 630 °C to approximately 650 °C. The temperature of the particles at low pressure is about 20 °C higher than that at atmospheric pressure in the later stage of the devolatilization, which is because there is less char formation and high temperature can be got with the same thermal supplement. Besides, the formation of more pores in the char reduces outward heat transfer from the particles, helping to maintain a relatively high temperature. As shown in Fig. 10(b), it is evident that the heating rate during the drying and devolatilization stages is significantly higher under lower environmental pressure with the same oxygen partial pressure. This is mainly attributed to the fact that the volatiles can release earlier, and oxidation of the volatiles takes place more significantly, resulting in a higher peak temperature of the char particles. Besides, as the pressure decreases, the heating process takes on a "step" character and an obvious subsection exists. This phenomenon is attributed to separating volatile ignition and combustion from the combustion of the char particles [51]. At low pressure, the early combustion of volatile components leads to a concentrated heat release, prompting temperature segmentation.

As shown in Fig. 10 (c), as the partial pressure decreases, the peak temperature decreases, and the temperature-fall period becomes smoother, indicating both the oxidation of the volatile matter and char are milder and combustion duration is prolonged in a low oxygen environment. In Fig. 10(d), as the pressure and oxygen partial pressure both decrease, the temperature of the particles will increase as a whole. Based on the previous analysis, it can be inferred that the combustion process in low-pressure, low-oxygen environments can be influenced by the heat and mass transfer between the particles and their surroundings.

From the above results, it can be known that the combustion process can be indeed influenced by the pressure and the partial pressure of oxygen. To investigate the mechanisms underlying the influence of pressure and oxygen on the particle combustion characteristics, a heat balance equation for the combustion of yak manure particles within the reactor is formulated [34,52,53]:

$$\rho_p V c_p \frac{dT_p}{dt} = q_L + h_g A_p (T_g - T_p) + q_{cfp} + q_{rfp} + q_{C-O_2} \quad (4)$$

in this equation, ρ, V, c, T, and A represent yak manure particles' density, volume, specific heat capacity, temperature, and surface area. The radiative heat input from the lamp cup is denoted as q_L. h_g stands for the convective heat transfer coefficient between the gas and particles. q_{cfp} indicates the convective heat transfer between the flame and particles. q_{rfp} corresponds to the radiative heat transfer between the flame and particles. Heat release from char oxidation is represented as $q_{C\text{-}O2}$. During the experiment, the temperature change of the particles is affected by the combination of radiant heat from the lamp cup, convective heat transfer between the flame and the particles, radiant heat transfer, and the heat of reaction of the combustion of the particles. The change of reaction pressure as well as oxygen concentration can change the diffusion ability of oxygen molecules in nitrogen, which can

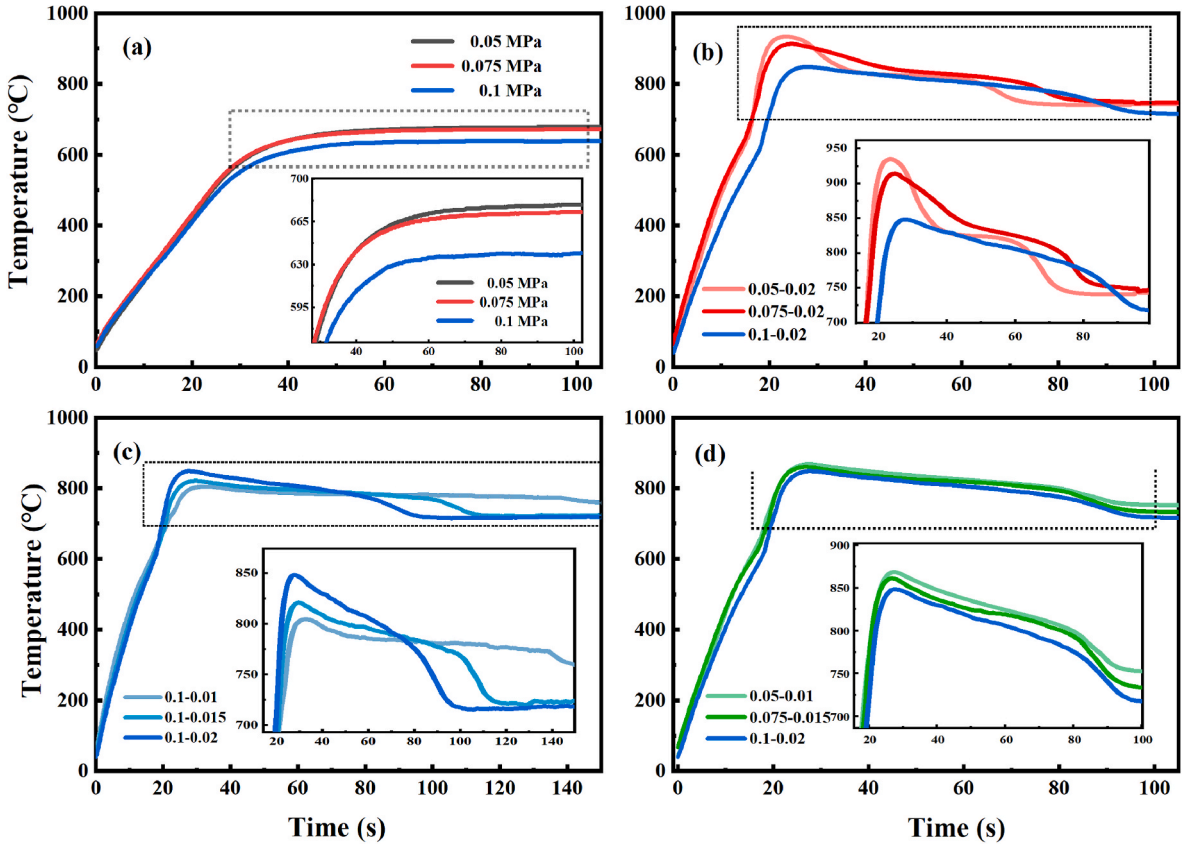

Fig. 10. Temperature during yak manure combustion at different pressures and oxygen contents.

have an effect on the physical properties of the gas, and also affect the pore structure of the particle, changing the particle thermal resistance and the heat transfer process, and affecting the heat balance of equation (4).

To facilitate comparison, Fig. 11 illustrates the characteristic temperatures of the particles under different conditions. This depiction enhances clarity and enables a more comprehensive comparison of particle behaviors under various conditions [54,55]. In Fig. 11(a), it is evident that with a decrease in environmental pressure, the ignition temperature, peak temperature, and burnout temperature of the particles all increase while the corresponding times decrease. This suggests that the combustion process of particles under low pressure becomes more compact and intense. Combining the heat balance equation (4) with Fig. 11(a), the following inferences can be readily drawn: low-pressure conditions promote the devolatilization and ignition of the volatile. The heat exchange between volatiles and particles (q_{cfp}, q_{rfp}) is more significant at lower pressures, resulting in earlier ignition of the particles. Besides, the low pressure promotes the development of the pore structure of the particles, resulting in a decrease in the specific heat capacity (c_p) of the particles and an increase in the rate of change of temperature (dT/dt) at the same time. In addition, the time required for complete combustion is shortened due to the separation of the volatile components from the char combustion process, weakening the interaction between the volatile components and the char.

As shown in Fig. 11(b), it can be observed that as the oxygen partial pressure in the atmosphere decreases, both the ignition temperature and the burnout temperature of the particles increase. In contrast, the peak temperature decreases, and the corresponding times all show an increase. This suggests that under low oxygen conditions, the combustion process of particles becomes milder. According to the analysis based on the heat balance equation, a low oxygen environment inhibits the reaction between oxygen molecules and the volatile matter and char, resulting in a slow release of $q_{C\text{-}O2}$. As a result, the ignition time and combustion time are prolonged, and the peak temperature of the particles is reduced.

As shown in Fig. 11(c), when low pressure and low oxygen interact simultaneously, the particles' ignition, peak, and burnout temperatures have an obvious increases and the corresponding times have slight decreases. It indicates that the combustion of yak manure has a slight ahead and the particle temperature increases under the low pressure and low oxygen conditions comparing to the atmospheric condition. It is a comprehensive effects of low pressure and low oxygen, and the impact of low-pressure on the combustion process outweighs that of low-oxygen conditions. For the change trends for the time of the characteristic temperatures, it is in consistent with the results in Fig. 3 from the pictures in Fig. 2. It is known that when the oxygen partial pressure decreases, the absolute amount of oxygen around the particle also decreases, which is not beneficial to ignition and combustion. However, for the combustion of yak manure at low pressure and low oxygen condition can still have a slight ahead combustion. It indicates that the effects of the low pressure on the release of the volatiles have a significant influence on the whole combustion process of yak manure at plateau section. The earlier and rapid release of the volatiles at low pressure condition can accelerate ignition. The well-developed internal pore structure and high surface area during devolatilization can promote the diffusion of the oxygen and thus the oxidation or combustion of the char, which can be further confirmed by an earlier CO formation and release in the gas during combustion at low pressure and low oxygen condition shown in Fig. S2. For the increased particle temperature during combustion at low pressure and low oxygen condition, it can be mainly attributed to the low specific heat capacity of char, and thus a higher temperature can maintain. Fig. S3 further shows the NO volume fraction during combustion of yak manure particles under different conditions. It reveals that an earlier and a lower peak value of NO was achieved during the combustion of yak manure at low pressure and low oxygen condition, which is beneficial to reduce and control the emission of NO.

3.4. The combustion mechanism of yak manure particles at the plateau region

In order to illustrate the effects of low pressure and low oxygen conditions on the combustion process of yak manure, the combustion mechanism of yak manure is shown in Fig. 12. The combustion process can be divided into three main stages: firstly, the yak manure particles are heated, and the temperature rises rapidly. The moisture can be released from the particle. With the temperature further increasing, alkanes, olefins, oxygen-containing functional groups, or side chains of aromatic rings begin to break and reorganize, and the volatiles began to release rapidly. The pores inside the particles begin to form. During this process, the space steric hindrance effect of the molecular network increases as more aromatic rings form, which leads to a rapid increase in the concentration of stable free radicals in the char. With the continuous release of the volatiles, the pore structure continues to develop. During these stages, the particles are surrounded by volatiles, and the oxidation of the volatiles can take place and consume the oxygen content in the atmosphere. Besides, the release of the volatile from the inside char also prevents the limited oxygen from coming into contact with the char.

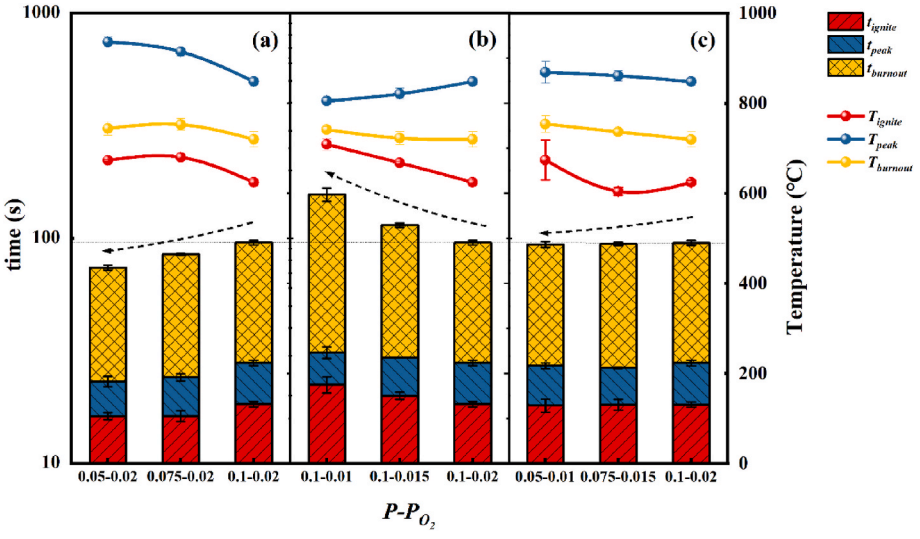

Fig. 11. The characteristic temperatures of particles under different conditions.

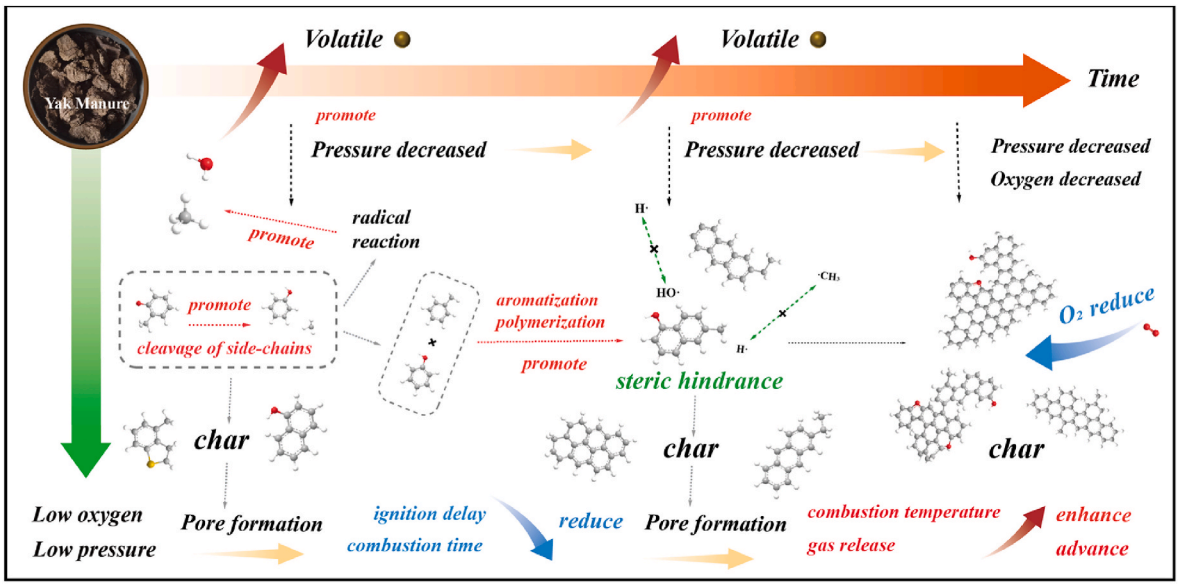

Fig. 12. Combustion mechanism of yak manure under low pressure and low oxygen condition.

Therefore, the char is hard to ignite. Finally, when the release and oxidation of the volatiles are finished, the char continues to burn until it is burned out.

Low-pressure and low-oxygen conditions significantly affect the combustion process of yak manure, and their influence varies depending on the specific conditions. When the pressure of the atmosphere is lower than the normal atmospheric pressure, the devolatilization process of the particles is enhanced, accelerating the cleavage of side chains and the formation of aromatic rings, leading to the creation of more porous structures. Additionally, under low-pressure conditions, the concentration of stable free radicals in the char increases significantly. These changes notably change the properties of the char, further lead to a char with lower weight and specific heat capacity, resulting in a higher combustion temperature of the char, an earlier ignition, and faster burnout. When the oxygen partial pressure in the atmosphere decreases with a constant environment pressure, the reaction between oxygen and volatiles or char would be inhibited, resulting in a prolonged ignition time, lower peak temperatures of the particles, and harder burnout.

When the partial pressure of oxygen and the total ambient pressure were simultaneously reduced, the earlier and rapid release of the volatiles at low pressure condition can counteract the effects of low oxygen and accelerate ignition, resulting in the shortened ignition delay comparing to the atmospheric combustion. Besides, the well-developed internal pore structure and high surface area of the char during devolatilization in the low pressure condition can promote the diffusion of the oxygen, and also result in a low specific heat capacity of char, enhancing the combustion temperature, thus further promote the oxidation or combustion of the char, counteracting the effects of low oxygen, resulting in a slight lower combustion time comparing to the atmospheric combustion. Besides, as there is an earlier volatile release and ignition, the combustion period is spread, and thus the peak value of the CO and NO is lower. This characteristic holds significant implications for enhancing combustion efficiency and pollutant control in industrial applications. It can effectively reduce the emission of harmful gases, particularly in the areas of ash handling and NO emission control, thereby improving environmental quality and enhancing the eco-friendliness of the combustion process.

4. Conclusion

This study investigated the devolatilization and combustion characteristics of yak manure particles under low pressure and low oxygen conditions in a concentrating photothermal combustion experimental system. The effects, characteristics, and mechanisms of low pressure and low oxygen on the devolatilization and combustion process of yak manure in plateau areas were discussed and analyzed. The main conclusions can be drawn as follows:

(1) Pressure significantly affects the devolatilization and combustion process. Low pressure promotes the devolatilization process of the particles, accelerate the breakage of side chains and the formation of the aromatic rings, form more pores, and increase the concentration of stable free radicals in the char. This leads to a char with lower weight and specific heat capacity, resulting in a higher combustion temperature of the char, an earlier ignition, and faster burnout.
(2) When both pressure and oxygen content are reduced under plateau conditions, they jointly influence the combustion process of yak manure, showing a competitive effect. The well-developed internal pore structure and high surface area of the char promote oxygen diffusion, while the low specific heat capacity of char formed under low-pressure conditions enhances combustion temperature. These factors can counteract the negative effects of low oxygen availability on the combustion process.
(3) Compared to atmospheric combustion, the combustion process of yak manure under simulated plateau conditions shows several distinct characteristics: shorter ignition and burnout times, higher particle combustion temperatures, and earlier but lower peak concentrations of CO and NO. These findings are critical and should be carefully considered in the design and operation of burners and combustors for industrial applications involving yak manure combustion in plateau regions.

CRediT authorship contribution statement

Bin Zhao: Writing – review & editing, Supervision. **Zihan Zhang:** Writing – original draft, Conceptualization. **Jun Xu:** Writing – review & editing, Supervision, Methodology, Funding acquisition. **Chenghong Liu:** Writing – review & editing. **Mengxia Qing:** Supervision. **Long Jiang:** Validation, Resources. **Yi Wang:** Methodology. **Song Hu:** Writing – review & editing, Supervision. **Zhongyang Luo:** Writing – review & editing, Supervision. **Jun Xiang:** Writing – review & editing, Supervision.

Acknowledgments

This work was supported by the National Natural Science Foundation of China (NSFC) (52176110, 52076097), the Key Research and Development Program of Hubei (2022BCA063), State Key Laboratory of Clean Energy Utilization Open Fund (ZJUCEU2023022) and Postgraduate Scientific Research Innovation Project of Hunan Province (CX20220928).

Appendix A. Supplementary data

Supplementary data to this article can be found online at https://doi.org/10.1016/j.biombioe.2025.107919.

Data availability

Data will be made available on request.

References

[1] P. Chen, S. Kang, J. Bai, M. Sillanpää, C. Li, Yak dung combustion aerosols in the Tibetan Plateau: chemical characteristics and influence on the local atmospheric environment, Atmos. Res. 156 (2015) 58–66, https://doi.org/10.1016/j.atmosres.2015.01.001.
[2] A.T. Kole, B.A. Zeru, E.A. Bekele, A.V. Ramayya, Design, development, and performance evaluation of husk biomass cook stove at high altitude condition, Int. J. Thermofluids 16 (2022) 100242, https://doi.org/10.1016/j.ijft.2022.100242.
[3] J.A. Rosati, K.Y. Yoneda, S. Yasmeen, S. Wood, M.W. Eldridge, Respiratory health and indoor air pollution at high elevation, Arch. Environ. Occup. Health 60 (2005) 96–105, https://doi.org/10.3200/AEOH.60.2.96-105.
[4] B. Winterhalder, R. Larsen, R.B. Thomas, Dung as an essential resource in a highland Peruvian community, Hum. Ecol. 2 (1974) 89–104, https://doi.org/10.1007/BF01558115.
[5] C. Yang, G. Tsedan, Q. Fan, S. Wang, Z. Wang, S. Chang, et al., Behavioral patterns of yaks (Bos grunniens) grazing on alpine shrub meadows of the Qinghai-Tibetan Plateau, Appl. Anim. Behav. Sci. 234 (2021) 105182, https://doi.org/10.1016/j.applanim.2020.105182.
[6] G. Chen, K. Gao, B. Yan, Z. Dan, W. Zhou, Z. Cheng, Estimation and emissions from crop straw and animal dung in Tibet, Sci. Total Environ. 631–632 (2018) 1038–1045, https://doi.org/10.1016/j.scitotenv.2018.03.029.
[7] X. Shen, G. Huang, Z. Yang, L. Han, Compositional characteristics and energy potential of Chinese animal manure by type and as a whole, Appl. Energy 160 (2015) 108–119, https://doi.org/10.1016/j.apenergy.2015.09.034.
[8] J. Fermoso, O. Mašek, Thermochemical decomposition of coffee ground residues by TG-MS: a kinetic study, J. Anal. Appl. Pyrolysis 130 (2018) 358–367, https://doi.org/10.1016/j.jaap.2017.12.007.
[9] Y. Xin, D. Wang, X.Q. Li, Q. Yuan, H. Cao, Influence of moisture content on cattle manure char properties and its potential for hydrogen rich gas production, J. Anal. Appl. Pyrolysis 130 (2018) 224–232, https://doi.org/10.1016/j.jaap.2018.01.005.
[10] Z. Fu, Y. Xue, J. Li, B. Yan, Z. Han, G. Chen, Steam gasification of yak manure: kinetic modeling by a sequential and coupling method, Fuel 329 (2022) 125464, https://doi.org/10.1016/j.fuel.2022.125464.
[11] Q. Wang, Prevention of Tibetan eco-environmental degradation caused by traditional use of biomass, Renew. Sustain. Energy Rev. 13 (2009) 2562–2570, https://doi.org/10.1016/j.rser.2009.06.013.
[12] Ronggui Tang, Ziyin Du, Gaodi Zhu, Yunying Fang, EI-Naggar Ali, Bhupinder Pal Singh, et al., Yak dung pat fragmentation decreases yield-scaled growing-season nitrous oxide emissions in an alpine steppe on the Qinghai-Tibetan Plateau, Biol. Fertil. Soils 57 (2021) 1103–1115, https://doi.org/10.1007/s00374-021-01601-0.
[13] S.R. Shewchuk, A. Mukherjee, A.K. Dalai, Selective carbon-based adsorbents for carbon dioxide capture from mixed gas streams and catalytic hydrogenation of CO2 into renewable energy source: a review, Chem. Eng. Sci. 243 (2021) 116735, https://doi.org/10.1016/j.ces.2021.116735.
[14] J. Zhang, Kinetics, thermodynamics, gas evolution and empirical optimization of cattle manure combustion in air and oxy-fuel atmospheres, Appl. Therm. Eng. 149 (2019) 119–131, https://doi.org/10.1016/j.applthermaleng.2018.12.010.
[15] J. Zhang, G. Sun, J. Liu, F. Evrendilek, M. Buyukada, Co-combustion of textile dyeing sludge with cattle manure: assessment of thermal behavior, gaseous products, and ash characteristics, J. Clean. Prod. 253 (2020) 119950, https://doi.org/10.1016/j.jclepro.2019.119950.
[16] S. Zhou, X. Chen, H. Zhang, H. Liu, The influence of combustion temperature on alkali content of cattle manure ash, Case Stud. Constr. Mater. 14 (2021) e00519, https://doi.org/10.1016/j.cscm.2021.e00519.
[17] G. Chen, S. He, Z. Cheng, Y. Guan, B. Yan, W. Ma, et al., Comparison of kinetic analysis methods in thermal decomposition of cattle manure by themogravimetric analysis, Bioresour. Technol. 243 (2017) 69–77, https://doi.org/10.1016/j.biortech.2017.06.007.
[18] X. Yuan, T. He, H. Cao, Q. Yuan, Cattle manure pyrolysis process: kinetic and thermodynamic analysis with isoconversional methods, Renew. Energy 107 (2017) 489–496, https://doi.org/10.1016/j.renene.2017.02.026.
[19] M. Ashraf, N. Ramzan, R.U. Khan, A.K. Durrani, Analysis of mixed cattle manure: kinetics and thermodynamic comparison of pyrolysis and combustion processes, Case Stud. Therm. Eng. 26 (2021) 101078, https://doi.org/10.1016/j.csite.2021.101078.
[20] C. Jiang, Q. Lin, C. Wang, X. Jiang, H. Bi, L. Bao, Experimental study of the ignition and combustion characteristics of cattle manure under different environmental conditions, Energy 197 (2020) 117143, https://doi.org/10.1016/j.energy.2020.117143.
[21] A. Song, F. Zha, X. Tang, Y. Chang, Effect of the additives on combustion characteristics and desulfurization performance of cow dung briquette, Chem. Eng. Process.Process Intensif. 143 (2019) 107585, https://doi.org/10.1016/j.cep.2019.107585.
[22] X. Hu, Y. He, Z. Li, J. Wang, Combustion characteristics of n-heptane at high altitudes, Proc. Combust. Inst. 33 (2011) 2607–2615, https://doi.org/10.1016/j.proci.2010.07.025.
[23] W. Yao, X. Hu, J. Rong, J. Wang, H. Zhang, Experimental study of large-scale fire behavior under low pressure at high altitude, J. Fire Sci. 31 (2013) 481–494, https://doi.org/10.1177/0734904113481326.
[24] C. Ding, Z. Yan, Y. Li, L. He, S. Ma, X. Wang, et al., Effect of pressure and stacking method on combustion characteristics of paper stacks, Case Stud. Therm. Eng. 38 (2022) 102375, https://doi.org/10.1016/j.csite.2022.102375.
[25] J. Dai, L. Yang, X. Zhou, Y. Wang, Y. Zhou, Z. Deng, Experimental and modeling study of atmospheric pressure effects on ignition of pine wood at different altitudes, Energy Fuel. 24 (2010) 609–615, https://doi.org/10.1021/ef900781m.
[26] W. Wang, L. Wang, R. Yang, H. Zhang, C. Ren, J. Yang, Investigation of the effect of low pressure on fire hazard in cargo compartment, Appl. Therm. Eng. 158 (2019) 113775, https://doi.org/10.1016/j.applthermaleng.2019.113775.
[27] T. Yamazaki, T. Matsuoka, K. Kuwana, Y. Nakamura, Study on the flaming-transition behavior of a downwardly smoldering biomass stick utilizing low pressure, Proc. Combust. Inst. 38 (2021) 5073–5080, https://doi.org/10.1016/j.proci.2020.07.100.
[28] T.F. Wall, G. Liu, H. Wu, D.G. Roberts, K.E. Benfell, S. Gupta, et al., The effects of pressure on coal reactions during pulverised coal combustion and gasification, Prog. Energy Combust. Sci. 28 (2002) 405–433, https://doi.org/10.1016/S0360-1285(02)00007-2.
[29] C. Wang, M. Lei, W. Yan, S. Wang, L. Jia, Combustion characteristics and ash formation of pulverized coal under pressurized oxy-fuel conditions, Energy Fuel. 25 (2011) 4333–4344, https://doi.org/10.1021/ef200956q.
[30] J. Fermoso, M.V. Gil, A.G. Borrego, C. Pevida, J.J. Pis, F. Rubiera, Effect of the pressure and temperature of devolatilization on the morphology and steam gasification reactivity of coal chars, Energy Fuel. 24 (2010) 5586–5595, https://doi.org/10.1021/ef100877t.
[31] D. Zeng, M. Clark, T. Gunderson, W.C. Hecker, T.H. Fletcher, Swelling properties and intrinsic reactivities of coal chars produced at elevated pressures and high heating rates, Proc. Combust. Inst. 30 (2005) 2213–2221, https://doi.org/10.1016/j.proci.2004.07.038.
[32] D. Lin, L. Liu, Y. Zhao, Y. Zhao, P. Qiu, X. Xie, et al., Influence of pyrolysis pressure on structure and combustion reactivity of Zhundong demineralized coal char, J. Energy Inst. 93 (2020) 1798–1808, https://doi.org/10.1016/j.joei.2020.03.011.
[33] D. Lin, Physicochemical structure characteristics and intrinsic reactivity of demineralized coal char rapidly pyrolyzed at elevated pressure, J. Energy Inst. (2020).
[34] L. Li, L. Duan, Z. Yang, C. Zhao, Pressurized oxy-fuel combustion characteristics of single coal particle in a visualized fluidized bed combustor, Combust. Flame 211 (2020) 218–228, https://doi.org/10.1016/j.combustflame.2019.09.032.
[35] J. Yan, M. Fang, T. Lv, X. Sun, Y. Zhu, J. Cen, et al., Pressurized oxy-fuel combustion of pulverized coal blended with wheat straw: thermochemical characterization and synergetic effect, J. Energy Inst. 108 (2023) 101237, https://doi.org/10.1016/j.joei.2023.101237.
[36] H. Li, H. Chi, S. Hu, G. Song, H. Leong, K. Xu, et al., Effect of oxygen concentration on combustion behavior of single coal pellets from three different ranks in a concentrating photothermal reactor, Fuel 269 (2020) 117372, https://doi.org/10.1016/j.fuel.2020.117372.
[37] G. Song, D. Huang, H. Li, X. Wang, Q. Ren, L. Jiang, et al., Pyrolysis reaction mechanism of typical Chinese agriculture and forest waste pellets at high heating rates based on the photo-thermal TGA, Energy 244 (2022) 123164, https://doi.org/10.1016/j.energy.2022.123164.
[38] D. Chen, J. Xu, P. Ling, Z. Fang, Q. Ren, K. Xu, et al., Formation and evolution mechanism of persistent free radicals in biochar during biomass pyrolysis: insights from biochar's element composition and chemical structure, Fuel 357 (2024) 129910, https://doi.org/10.1016/j.fuel.2023.129910.
[39] J. Xu, Q. He, Z. Xiong, Y. Yu, S. Zhang, X. Hu, et al., Raman spectroscopy as a versatile tool for investigating thermochemical processing of coal, biomass, and wastes: recent advances and future perspectives, Energy Fuel. 35 (2021) 2870–2913, https://doi.org/10.1021/acs.energyfuels.0c03298.
[40] X. Wang, Q. Chen, H. Zhu, X. Chen, G. Yu, In-situ study on structure evolution and gasification reactivity of biomass char with K and Ca catalysts at carbon dioxide atmosphere, Carbon Resour. Convers. 6 (2023) 27–33, https://doi.org/10.1016/j.crcon.2022.10.002.
[41] M. Asadullah, S. Zhang, Z. Min, P. Yimsiri, C.-Z. Li, Effects of biomass char structure on its gasification reactivity, Bioresour. Technol. 101 (2010) 7935–7943, https://doi.org/10.1016/j.biortech.2010.05.048.

[42] Y. Chen, S.S.A. Syed-Hassan, Z. Deng, X. Hu, J. Xu, L. Jiang, et al., Effects of aspect ratio on char structure during the pyrolysis of sawdust pellet, Fuel 325 (2022) 124850, https://doi.org/10.1016/j.fuel.2022.124850.
[43] Y. Chen, S.S.A. Syed-Hassan, Z. Xiong, Q. Li, X. Hu, J. Xu, et al., Temporal and spatial evolution of biochar chemical structure during biomass pellet pyrolysis from the insights of micro-Raman spectroscopy, Fuel Process. Technol. 218 (2021) 106839, https://doi.org/10.1016/j.fuproc.2021.106839.
[44] X. Li, J. Hayashi, C. Li, FT-Raman spectroscopic study of the evolution of char structure during the pyrolysis of a Victorian brown coal, Fuel 85 (2006) 1700–1707, https://doi.org/10.1016/j.fuel.2006.03.008.
[45] Y. Chen, Z. Deng, Q. Ren, D. Ren, S. Su, S. Hu, et al., Evolution of char structure during the pyrolysis of biomass pellet: further understanding on the effects of chars two phases, Fuel 312 (2022) 122994, https://doi.org/10.1016/j.fuel.2021.122994.
[46] H. Yang, Correlation between pores and chemical structures in CO2 gasification char of Naomaohu coal, Combust. Flame (2023).
[47] H. Meng, Co-pyrolysis of platanus wood and bituminous coal: product distributions, char pore analysis and synergistic effects, J. Anal. Appl. Pyrolysis (2022).
[48] J. Xu, J. Liu, P. Ling, X. Zhang, K. Xu, L. He, et al., Raman spectroscopy of biochar from the pyrolysis of three typical Chinese biomasses: a novel method for rapidly evaluating the biochar property, Energy 202 (2020) 117644, https://doi.org/10.1016/j.energy.2020.117644.
[49] L. Ma, S.S.A. Syed-Hassan, J. Zhou, W. Deng, Y. Xiong, X. Wang, et al., Effect of alkali and alkali earth metals on reactions of stable free radicals during biomass pyrolysis: an in-situ EPR study, Fuel Process. Technol. 250 (2023) 107916, https://doi.org/10.1016/j.fuproc.2023.107916.
[50] Z. Ma, Y. Yang, Q. Ma, H. Zhou, X. Luo, X. Liu, et al., Evolution of the chemical composition, functional group, pore structure and crystallographic structure of biochar from palm kernel shell pyrolysis under different temperatures, J. Anal. Appl. Pyrolysis 127 (2017) 350–359, https://doi.org/10.1016/j.jaap.2017.07.015.
[51] L. Hanjian, C. Huanying, H. Song, H. Limo, X. Kai, M.E. Mostafa, et al., Combustion behavior of large size coal over a wide range of heating rates in a concentrating photothermal reactor, Fuel Process. Technol. 197 (2020) 106187, https://doi.org/10.1016/j.fuproc.2019.106187.
[52] C. Bu, A. Gómez-Barea, X. Chen, B. Leckner, D. Liu, D. Pallarès, et al., Effect of CO2 on oxy-fuel combustion of coal-char particles in a fluidized bed: modeling and comparison with the conventional mode of combustion, Appl. Energy 177 (2016) 247–259, https://doi.org/10.1016/j.apenergy.2016.05.108.
[53] J. Salinero, A. Gómez-Barea, D. Fuentes-Cano, B. Leckner, Measurement and theoretical prediction of char temperature oscillation during fluidized bed combustion, Combust. Flame 192 (2018) 190–204, https://doi.org/10.1016/j.combustflame.2018.02.005.
[54] R. Jovanovic, A. Milewska, B. Swiatkowski, A. Goanta, H. Spliethoff, Numerical investigation of influence of homogeneous/heterogeneous ignition/combustion mechanisms on ignition point position during pulverized coal combustion in oxygen enriched and recycled flue gases atmosphere, Int. J. Heat Mass Tran. 54 (2011) 921–931, https://doi.org/10.1016/j.ijheatmasstransfer.2010.10.011.
[55] H. Li, H. Chi, S. Hu, G. Song, S. Abdulmajid Abdullahi, K. Xu, et al., Ignition of large size coal in a gas-phase temperature adjustable concentrating photothermal reactor: the influence of volumetric reactions, Fuel Process. Technol. 213 (2021) 106642, https://doi.org/10.1016/j.fuproc.2020.106642.